RAPID COMMUNICATIONS

PHYSICAL REVIEW B VOLUME 51, NUMBER 23 15 JUNE 1995-I

Collective transport in two-dimensional magnetic bubble arrays

Junmin Hu and R. M. Westervelt
Division of Applied Sciences and Department of Physics, Harvard University, Cambridge, Massachusetts 02138
(Received 7 February 1995)

We report detailed observations of transport in two-dimensional magnetic bubble arrays subject to random substrate pinning. Temperature is simulated via agitation with an ac magnetic field. The velocity-force responses follow power laws $v \propto F^{\alpha}$ with $\alpha \cong 3$. The bubble velocities under an applied force deviate from a simple Gaussian distribution, and the flow pattern shows nontrivial spatial correlations. The measured velocity-velocity correlation function decays exponentially, and the correlation length ξ_v increases with the applied force F.

Collective transport has attracted much theoretical and experimental attention.[1] Interesting and important spatiotemporal phenomena arise in a wide variety of different contexts due to the competition between internal ordering forces and external disorder.[1] The motion of elastic media subject to weak random pinning is of particular importance in fields ranging from mechanical friction[2,3] and earthquakes,[4] to charge-density-wave depinning and flux flow in type-II superconductors.[1] Due to the breadth of the range of applications, new results can have importance in quite different areas. A recent theory[5] of particular relevance to the present work describes the motion of an elastic two-dimensional membrane subject to weak random-point pinning, as well as charge-density-wave transport. Because extended systems can show a wide range of complex behavior, detailed theoretical assumptions concerning the spatiotemporal nature of transport are necessary to make progress. Often these assumptions are not directly tested in experiments because spatially and temporally resolved observations of collective motion are often difficult to carry out.

In this paper we report detailed spatiotemporal observations of collective transport in two-dimensional magnetic bubble arrays. Using computer-video techniques we visualize the motion of individual bubbles in an array subject to random pinning and study the spatiotemporal mechanism for depinning and motion. Thermal motion is simulated by an adjustable ac magnetic field which agitates individual bubbles. A series of measurements was made in the nonlinear regime of low bubble velocities to study how depinning occurs at finite temperatures. The observed average velocity versus force responses follow power laws $v \propto F^{\alpha}$ with $\alpha \cong 3$. Thresholded spatial images of bubble velocity distributions demonstrate how the array moves in response to the applied force. The velocity-velocity correlation function decays exponentially and the velocity-velocity correlation length increases with applied force.

For a two-dimensional array subject to a random pinning potential, a depinning threshold only exists at zero temperature;[6] at finite temperatures the array velocity is predicted to be nonzero for any applied force. The spatially averaged velocity v of an extended system given by collective flux creep theory[7] is activated:

$$v \propto e^{-U(F)/k_B T} \tag{1}$$

below a critical temperature T_c. Above T_c the velocity-force response is predicted to be linear. The energy barrier $U(F)$ in Eq. (1) is associated with the nature of the collective motion. In the three-dimensional case[6,7] $U(F) \propto F^{-\nu}$ which leads to a strongly nonlinear response of the form $v \propto e^{-(F_0/F)^{\nu}}$. For the experiments below, the relevant case is a defect-free two-dimensional elastic medium under weak random-point pinning: here the balance between elastic energy and pinning gives an energy barrier of the form $U(F) \propto \ln(F/F_0)$ that leads to power-law velocity-force responses[5,8]

$$v \propto F^{\alpha}. \tag{2}$$

The instantaneous velocity-velocity correlation function is predicted to decay exponentially with separation at zero temperature:[1]

$$C(r_{ij}) = \left\langle \left(\frac{\partial x_i}{\partial t} - v \right) \left(\frac{\partial x_j}{\partial t} - v \right) \right\rangle \propto \exp(-|\mathbf{r}_i - \mathbf{r}_j|/\xi_v), \tag{3}$$

where $\mathbf{r}_i$ is the position of site i and v is the spatial average velocity, assumed to be in the x direction. The correlation length ξ_v characterizes the size of regions that move coherently.

Our experiments are conducted on arrays of magnetic bubbles, which are cylindrical domains of reversed perpendicular magnetization in a thin uniaxial ferrimagnetic garnet film. Bubble arrays can be regarded as two-dimensional elastic media composed of discrete objects pinned by weak point disorder. A well-annealed bubble array in good quality garnet material forms a two-dimensional triangular array with few dislocations.[9] Bubbles interact via a repulsive dipole-dipole potential. Microscopic substrate roughness and random-alloy fluctuations[10] produce a random potential on length scales much shorter than the bubble radius, which can be considered weak random-point disorder.[11] The effect of temperature is simulated in our experiments by a superimposed ac magnetic field. The breathing motion of bubbles in response to the ac field interacts with substrate roughness to produce random Brownian motion and an effective temperature.[11] The magnetic energy density of a perfect bubble lattice has been calculated by Cape and Lehman,[12] assuming the shape of a bubble is exactly cylindrical, and can be used to com-

0163-1829/95/51(23)/17279(4)/$06.00

pute the bubble-bubble forces and the Lamé coefficients μ and λ.[13] Interestingly, magnetic bubbles possess an effective inertial mass due to domain-wall motion,[12] which is quite small ($m \sim 10^{-16}$ g) for most materials.

The sample used in these experiments is a rare-earth iron garnet film of size 6×25 mm^2 with chemical composition $(Bi_{1.09}Tm_{0.07}Gd_{0.95}Y_{0.90})(Fe_{3.91}Ga_{0.76}Y_{0.30}Tm_{0.02})O_{12}$ grown on a nonmagnetic garnet substrate. The film has a thickness 7.8 μm, and saturation magnetization $4\pi M_s = 190$ G. An array of magnetic bubbles is produced by briefly inserting the sample into a strong (2.5 kG) in-plane magnetic field, followed by annealing in an ac magnetic field to reduce the number of structural defects. A perpendicular dc magnetic field H_{dc} is applied to control the bubble concentration; for the data below, $H_{dc} = 75$ Oe, the bubble concentration is 2996 mm^{-2}, and the bubble diameter is 6 μm. The resulting bubble array is well ordered: the dislocation concentration is low, the array has long-range orientational order, and the measured translational correlation length is relatively long, $8a-15a$, where a is the average bubble spacing. The Lamé coefficients for these parameters are calculated to be $\lambda \cong 30$ erg/cm^2, $\mu \cong 10$ erg/cm^2. The effect of temperature is simulated by a superimposed perpendicular ac magnetic field with adjustable peak-to-peak amplitude H_{ac} and frequency 40 Hz; the ac field produces a periodic change in bubble radius which interacts with substrate roughness to produce random motion.[11] In order to study transport, a uniform in-plane force on each bubble is generated by an in-plane gradient in the perpendicular magnetic field, produced using a pair of gradient coils. The apparatus is placed on a mechanically isolated optical table to minimize vibration.

The motion of individual bubbles in the array is visualized via the Faraday rotation of polarized light in a precision optical microscope, recorded onto video tape, and analyzed with computer-video techniques on a Silicon Graphics workstation. Each image below contains about 2700 bubbles and covers part of a single crystallite of the polycrystalline bubble array. Image analysis is used to locate the bubble centers with accuracy $\cong 0.2$ μm. The velocity of each bubble is determined from its displacement over subsequent video frames, and the array velocity v is computed by averaging over all the bubbles in the field of view. Collective transport data are recorded by applying an in-plane force and observing the resulting motion, then removing the force and allowing the array to relax. The duration of the measurement is limited by compression of the bubble array in the entire sample, which builds up in time in the direction opposing the applied force. For array displacements up to $3a$ used in this experiment, no changes in the characteristics of bubble motion are observed: the translational and orientational order both remain unchanged. This distance is a factor ~ 100 longer than the length scale of the random pinning (~ 0.4 μm) determined by the diffusion of isolated bubbles.[11]

Figures 1(a) and 1(b) are linear and log-log plots of the measured array velocity v versus applied force F for four values of the ac magnetic field H_{ac}. In absence of an ac field, the array is pinned within the available range of applied force. As shown, the velocity-force response is nonlinear, but does not display a threshold for array motion, in agreement with current theory for two dimensions.[5] The solid curves in Fig. 1(a) are fits to $v = cF^3$, with c the fitting parameter. We

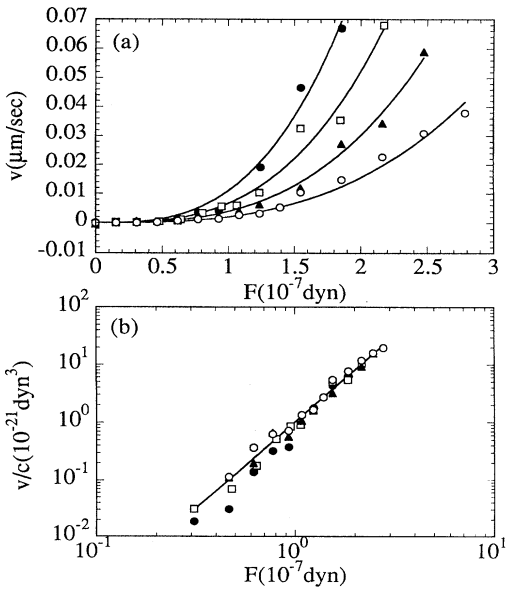

FIG. 1. (a) Velocity-force response of the magnetic bubble array for ac magnetic-field values $H_{ac} = 10.1$ Oe (open circles), 13.6 Oe (black triangles), 17.2 Oe (open squares), and 20.7 Oe (black circles). The solid lines are power-law fits with $v = cF^3$; c is the fitting parameter. (b) Log-log plot of v/c vs F; the solid line is $v/c = F^3$.

can look at the scaling behavior in Fig. 1(b), where all the points fall onto the same line $v/c = F^3$ on a log-log plot over three decades in velocity. Power-law velocity force characteristics are predicted for defect-free elastic media,[5] and also for certain cases in two dimensions due to the interaction of dislocations.[6] Elastic media theory is more appropriate to our experiments because the measured dislocation concentration of the bubble array is very small, ~ 4 over the field of view, and because we observe that the few dislocations present are fixed in the array. The effective temperature of isolated bubbles can be measured via the Einstein relation[11] because they diffuse freely in ac fields comparable to those in the present experiment and the drift velocity is proportional to the applied force. In an array, bubble diffusion is restricted and the situation is more complex. We characterize effective thermal fluctuations in bubble motion produced by H_{ac} via measurements of the standard deviation σ of the bubble displacement over 24 min in the absence of applied force. For Fig. 1 we find similar values $\sigma/a = 0.039 \pm 0.004$ for the four ac fields: as H_{ac} increases the array moves more freely, but the effective temperature represented by σ/a does not increase appreciably.

Spatial images of the moving array and corresponding velocity distributions are shown in Figs. 2(a)–2(c) for three increasing values of applied force. The bubble velocities are obtained from the displacements by dividing by the measurement interval $\Delta t = 2$ min, chosen long enough to minimize random fluctuations, yet short enough so that the displacement is smaller than the bubble separation a. Shown on the right-hand side of Fig. 2 are histograms of the bubble velocity distribution. In absence of a gradient force, the distribution is approximately Gaussian, associated with thermal fluc-

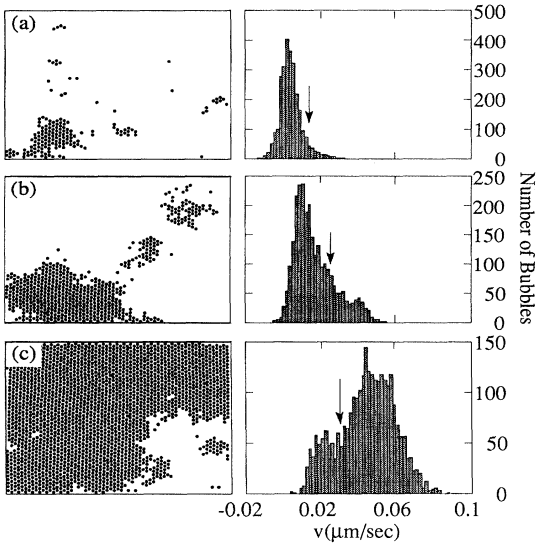

FIG. 2. Distributions of moving bubble clusters and histograms of bubble velocity for $H_{ac}=10.1$ Oe and (a) $F=0.93\times10^{-7}$ dyn, (b) $F=1.86\times10^{-7}$ dyn, and (c) $F=2.79\times10^{-7}$ dyn. The black dots represent bubbles with velocities above the cutoffs indicated by the arrows on the corresponding histograms. Image sizes are all 1027×768 μm^2.

tuations generated by the ac field. With an applied force, the velocity distribution deviates from a simple Gaussian as shown, developing nonthermal tails and bimodal structure. The corresponding spatial motion of the array is shown on the left-hand side in Fig. 2, by plotting as black dots bubbles with velocity above a cutoff indicated by the arrow in the histogram to the right. For Figs. 2(a) and 2(b) the cutoff velocity is chosen to be two standard deviations to the main peak, and for Fig. 2(c) the cutoff is chosen in the valley between the two maxima of the bimodal distribution. As shown, the array moves via the correlated displacement of groups of adjacent bubbles; the size of the displaced region increases with applied force. Much of the random bubble

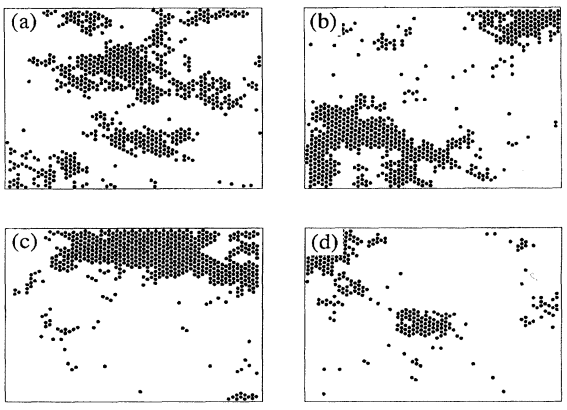

FIG. 3. Sequence of moving bubble images (1027×768 μm^2) for $H_{ac}=10.1$ Oe and $F=1.24\times10^{-7}$ dyn. The cutoff velocity is 0.0075 μm/sec. Each image is averaged over 6 min.

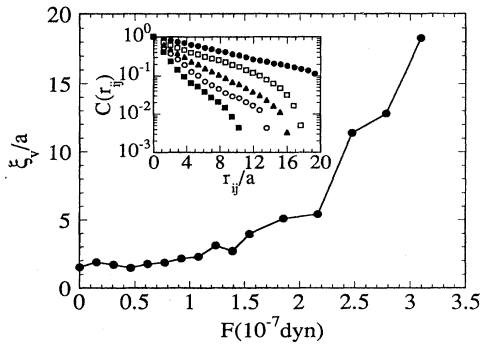

FIG. 4. Velocity-velocity correlation length ξ_v vs force F at $H_{ac}=10.1$ Oe. The inset shows the velocity-velocity correlation function vs bubble separation at forces 2.79×10^{-7} dyn (black dots), 1.86×10^{-7} dyn (open squares), 1.24×10^{-7} dyn (black triangles), 0.93×10^{-7} dyn (open circles), and 0.46×10^{-7} dyn (black squares).

motion produced by ac agitation is suppressed by thresholding. In Fig. 2(a) the small high velocity tail in the distribution corresponds to one small cluster of bubbles as shown. In Fig. 2(b) the force is larger, and the high velocity tail is bigger corresponding to three clusters. In Fig. 2(c) the distribution is bimodal: the higher velocity peak corresponds to a single spatially correlated part of the moving array as shown. From the images and histograms of the bubble velocities, it is clear that the motion is a collective phenomenon produced by correlated bubble displacements that are nonuniform across the array at a given time. The array motion is not simply a consequence of the random motion of individual bubbles, because the velocity distribution becomes distinctly non-Gaussian.

To understand how spatially nonuniform motion over the short times in Fig. 2 produces a uniform flow over longer times, we recorded a sequence of time-resolved images of the bubble flow, shown in Figs. 3(a)–3(d). The force was applied for a total of 24 min corresponding to a total displacement of the array by 4.6 μm; each image represents the motion over 6 min. The measured velocity distributions corresponding to Figs. 3(a)–3(d) each possess a high velocity tail. As before the images were thresholded with cutoff velocity 0.075 μm/sec. Averaged over 24 min, the motion is very uniform, and the measured velocity distribution is a good fit to a Gaussian displaced by the array velocity, without a high velocity tail. Over shorter time scales, the motion is spatially nonuniform, as illustrated by the sequence in Figs. 3(a)–3(d). Quickly moving clusters of bubbles in Fig. 3(a) exert stress on neighboring slowly moving parts of the array. The quickly moving part of the array changes in location and shape from frame to frame in Figs. 3(a)–3(d) as the stress created by nonuniform motion is passed through the array, producing more uniform motion over longer time scales. Image analysis indicates that no creation or annihilation of dislocations occurs in Figs. 3(a)–3(d), or in other typical data for these conditions, and that the few dislocations present simply move with the array so that elastic medium theory is applicable. This type of motion is analogous in many ways to sliding charge-density waves.[1] As for charge-density waves, the velocity for wave propagation of

deformations is much faster than array motion. Höfelt[13] obtained the velocity of propagation for deformation of a triangular magnetic bubble lattice $v_p = \sqrt{(\lambda + 2\mu)/\rho}$, where ρ is the effective mass density due to domain-wall motion. For our bubble array $v_p \cong 3 \times 10^4$ cm/sec, much greater than the average array velocity.

Figure 4 shows the measured velocity-velocity correlation length ξ_v versus applied force F; the correlation length ξ_v characterizes the size of the correlated moving regions. The values of ξ_v were determined from the measured velocity-velocity correlation function $C(r_{ij})$ from Eq. (3), which is plotted versus bubble separation in the inset of Fig. 4 for five representative values of force listed in the figure caption. As shown, $C(r_{ij})$ decays exponentially; the drop at large separations is due to finite image size. The velocity for Fig. 4 is averaged over 2 min to reduce the influence of thermal motion. For a small applied force F, when the array velocity is small, the correlation length ξ_v is of the order of the lattice spacing a, and is associated with random bubble agitation by the ac field. As shown, the velocity-velocity correlation length ξ_v increases monotonically with applied force. Theories of collective transport[1] predict a range of possible behaviors for ξ_v versus force, including a divergence at the depinning threshold for zero temperature. The present experiments do not observe a peak in ξ_v, but it is possible that the range of applied forces is below a zero-temperature depinning threshold.[1]

We thank Roger Belt of Airtron Division of Litton Industries for the garnet samples and D. S. Fisher, D. R. Nelson, T. Hwa, J. Watson, C. Carraro, and O. Narayan for helpful discussions. The work was supported by NSF Grant No. DMR-94-00396 and ONR Contract No. N00014-95-1-0104.

[1] D. S. Fisher, in *Nonlinearity in Condensed Matter*, edited by A. P. Bishop *et al.* (Springer-Verlag, New York, 1987), and references therein.

[2] D. P. Vallette and J. P. Gollub, Phys. Rev. E **47**, 820 (1993).

[3] H. J. S. Feder and J. Feder, Phys. Rev. Lett. **66**, 2669 (1991).

[4] J. M. Carlson and J. S. Langer, Phys. Rev. Lett. **62**, 2632 (1989).

[5] G. G. Batrouni and T. Hwa, Phys. Rev. Lett. **72**, 4133 (1994); C. Carraro, T. Hwa, and D. R. Nelson (unpublished).

[6] D. S. Fisher, M. P. A. Fisher, and D. A. Huse, Phys. Rev. B **43**, 130 (1991); D. S. Fisher, *ibid.* **31**, 1396 (1985).

[7] M. V. Feigel'man *et al.*, Phys. Rev. Lett. **63**, 2303 (1989).

[8] Y.-C. Tsai and Y. Shapir, Phys. Rev. Lett. **69**, 1773 (1992).

[9] R. Seshadri and R. M. Westervelt, Phys. Rev. Lett. **66**, 2774 (1991); Phys. Rev. B **46**, 5150 (1992).

[10] A. H. Eschenfelder, *Magnetic Bubble Technology*, 2nd ed. (Springer-Verlag, Berlin, 1981).

[11] R. Seshadri and R. M. Westervelt, Phys. Rev. B **46**, 5142 (1992).

[12] J. A. Cape and G. W. Lehman, J. Appl. Phys. **42**, 5732 (1971).

[13] M. H. H. Höfelt, J. Appl. Phys. **44**, 414 (1973).